

Enhanced mechanical performance of reinforced concrete beams with nano-alumina: an experimental and analytical flexural study

Jeevakkumar Rangarajan¹ , Renganathan Mathisekaran¹

¹Anna University, University College of Engineering, Department of Civil Engineering, 620024, Tiruchirapalli, Tamil Nadu, India.

e-mail: rangarajanjeevakkumar@gmail.com, mathirenga88@gmail.com

ABSTRACT

The increased use of concrete in modern construction contributes significantly to global warming and pollution-related health risks due to increased CO₂ emissions. The use of nanoparticles in cement composites has attracted significant attention from researchers in recent years. In the field of material science, nanomaterial's are an emerging field. This study investigates the flexural behavior of reinforced concrete beams incorporating nano-Alumina. Experimental tests and analytical models were conducted to evaluate performance improvements. To enhance the mechanical qualities of concrete, the experiment looks at nanoparticles such Nano Alumina (NA) and one of the useful cementitious elements in cement. In concrete, cementitious material partially replaces nanoparticles and pozzolanic material. To calibrate the strength parameters, a range of concrete mixes, including M30, M40, and M50, were cured for 28, 56, and 90 days in water. For mixtures hardened after 28, 56, and 90 days, compressive, split tensile, and flexural strengths were evaluated. An SEM analysis of the microstructure of mortar fragments present in concrete was conducted to determine how well nanoparticles fill concrete cavities. Due to the inherent brittleness and low tensile strength of conventional concrete, nano-Alumina (NA) was incorporated to enhance the mechanical performance of reinforced concrete beams. NA, owing to its high surface area and superior pozzolanic activity, refines the microstructure and improves load-bearing capacity. This study experimentally and analytically investigates the flexural behavior of NA-modified beams, demonstrating significant improvements in strength, ductility, and crack resistance.

Keywords: Concrete Beams; Flexural Behaviour; Nano-Alumina; Microstructure; ABAQUS.

1. INTRODUCTION

Concrete is a key material used in engineering construction and is frequently used in areas such as water conservation and hydropower, marine coastlines, civil engineering, roadways, and bridges. Concrete is readily cracked under stress because it is fragile and has poor tensile strength [1]. Cracks appear quickly when the load is continually increased. The brittleness and weakness of concrete under stress are two of its major drawbacks. Stress causes concrete to crack quickly, and cracks develop over time when concrete is stressed [2]. A strengthening method has been proposed to overcome the concrete's disadvantages by mixing the concrete with random discrete fibers. In concrete, fibers such as carbon, glass, steel, and polypropylene can improve energy absorption and crack resistance. Several fibers are used to enhance concrete's tensile strength and energy absorption, such as carbon, glass, steel, and polypropylene [3]. Cracks are covered in fiber-reinforced concrete (FRC), which also has a higher degree of ductility. As a result of its high tensile load, FRC may be used to create thin and long-span structural elements. The tension performance of conventional concrete, including post peak strain capacity, split tensile strength, toughness, and flexural strength, is primarily improved by the addition of fibres [4]. Since the materials generated by nanotechnology have many unique features, nanotechnology may be used for development cycles and planning in many fields. Massive outflows will be avoided by the employment of nanoparticles in solids, and the application of heated protections will result in efficient cooling energy utilisation. The solid material has to be superior than traditional concrete in terms of execution and quality in order to be employed in the construction sector [5]. Cement substituted with nanoparticles is made by substituting nanoparticles of less than 30 nanometers for the shortfalls and pores of conventional concrete. There are a variety of Nanoparticles available, such as Nano silica, Alumina, Iron, Carbon cylinders, and Titanium dioxide. Nano particles have recently been investigated for using to overcome concrete's insufficient early-age compressive strength. In the right arrangement, Nano particles act as a filler to fill in voids between concrete grains and bring about a higher

packing density by occupying the voids between concrete grains [6]. When applied to cement-based materials as an additive, nano-SiO₂ (hence referred to as NS) encourages a pozzolanic reaction. It's frequently employed in cement-based products, and when it's added to concrete admixtures, it encourages a pozzolanic reaction. Wang [7] investigated how the performance of concrete made using road cement is affected by nanoparticles. The test findings demonstrated that concrete's compressive strength, flexural strength, and permeability resistance could all be increased by adding the right quantity of NS and TiO₂. For various concrete assessments, pozzolanic material like metakaolin and nanoparticles like Nano Alumina were partially replaced with concrete in the blends by 1% and 15%, respectively [8] reported that adding NS and Nano-Fe₂O₃ to cement mortar could facilitate hydration, increase slurry performance, and fill capillary pores. Steel fiber concrete was studied by Mustafa [9] under the influence of NS. Steel fiber reinforced concrete's compressive strength, splitting tensile strength, and flexural strength could be improved by adding NS.

The strength and workability of the material will enhance with the addition of a nanoparticle. Metakaolin, a mineral additive, will also produce superior results when used as a partial replacement for concrete. The concrete's microstructure is improved by the use of nanoparticles, which also prevent calcium hydroxide from being fixed via a pozzolanic reaction. Modifications to micro concrete composites enhance their mechanical, administrative, and functional qualities, helping to provide a more economically put together environment [10]. Despite prior studies on Nano-alumina's mechanical and durability qualities in concrete, this work focuses primarily on an experimental investigation done to assess the flexural response of reinforced concrete beams enhanced with conventional cement and Nano Alumina. Nano alumina was added to the volume of cement at different rates (1%, 2%, 3%, 4%, and 5%) to replace the natural river sand. As an alternative, Msand was added in several amounts (25, 50, 75, and 100%). While nano-materials have been widely studied for enhancing cementitious matrices, limited research has focused specifically on the influence of nano-Alumina on the flexural performance of reinforced concrete structural elements. Existing studies primarily address compressive strength improvements at the material level, with insufficient experimental and analytical investigations on full-scale beam behavior under flexural loading. This study addresses this gap by evaluating the mechanical and flexural performance of reinforced concrete beams incorporating nano-Alumina through comprehensive experimental testing and analytical modelling. The current study seeks to enhance the mechanical characteristics of concrete, the Crake pattern, and the mechanism of failure in RC beams with simply supported RC frames using high strength concrete mixes (M30, M40, and M50) grade of Nano concrete with three points loading.

2. MATERIALS AND METHODS

2.1. Materials

In the experimental investigation, regular Portland cement of grade 43 with qualities that complied with IS: 4031-1988 and IS: 8112-2013 was employed. Nano-Alumina was used as a replacement for cement in this experiment, while Msand replaced natural sand in the experiment [11]. Table 1 lists the chemical and physical properties.

Table 1: Properties of cement and nanoalumina.

S.NO	NANO ALUMINA		CEMENT	
	PROPERTY	VALUE	PROPERTY	
1	Purity %	99.9%	Purity %	
2	Molecular Formula	Al ₂ O ₃	Molecular Formula	
3	CaO	<0.018%	CaO	65.23
4	Fe ₂ O ₃	<0.034	Fe ₂ O ₃	2.73
5	MgO	<0.001%	MgO	1.82
6	SiO ₂	<0.05%	SiO ₂	22.90
7	Average Particle size	25–55 nm	Average Particle size	12 nm
8	Specific surface area (SSA)	110–130 m ² /g	Specific surface area (SSA)	38.5 m ² /g
9	True density	3.85 g/cm ³	True density	14.23 g/cm ³
10	Bulk density	1.75 g/cm ³	Bulk density	2.23 g/cm ³
11	pH	6–10	pH	7–12
12	Morphology	Spherical	Morphology	Spherical

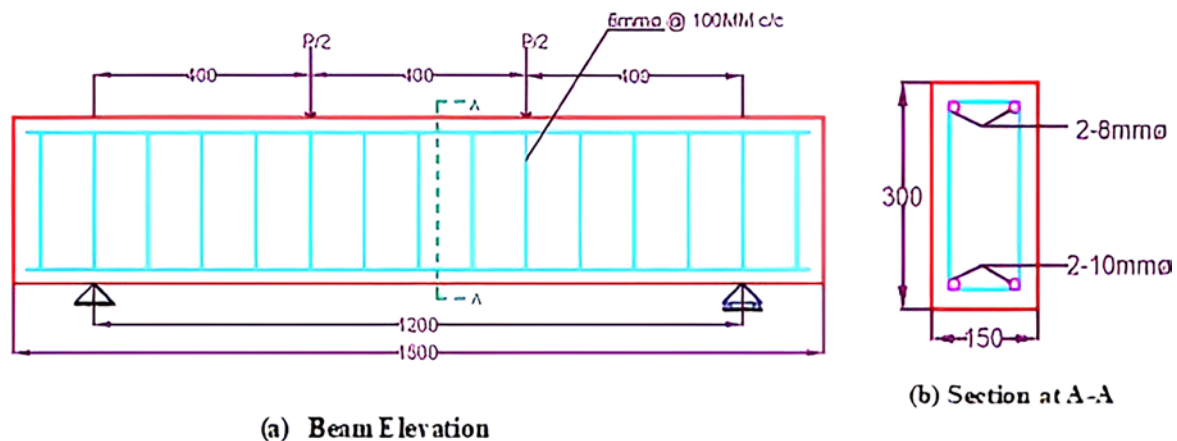
Table 2: Aggregate characteristics.

PROPERTY	RIVER SAND	MSAND	COARSE AGGREGATE
Specific Gravity	2.72	2.82	2.77
Bulk Density kg/m ³	149	1687	1587
Water Absorption	0.6	1.25	0.33
Void Content	36.87	29.84	48.42

Msand, which is created by impact crushing granite, takes the role of natural sand. The aggregate's physical characteristics are shown in Table 2. The fineness content of Msand is within the permitted range as established by Zone II of Indian Standards. Nano silica is high purity amorphous silica nanopowder with a sizable surface area and favourable dispersion characteristics. By speeding the hydration and pozzolanic processes early on, the addition of Nano silica to a lower cement replacement level boosts the mechanical and durability qualities of concrete. Despite having a vast surface area, Nano Alumina tends to aggregate. Before being introduced to a wet mixture, nanomaterials need to be ultrasonically and with a surfactant agglomerated.

3. AN OVERVIEW OF CONCRETE SPECIMEN PREPARATION

Cement and sand were mixed for about two minutes in a pan mixer to prepare concrete specimens with nano particles for different grades. Nano particles were stirred at 350 rpm for about 5 minutes at a rate of 350 rpm for about 5 minutes for uniform dispersion of the chemical admixture without coagulating. The remaining 70% of water was then added to the dry mixture, and the mixture was then constantly stirred for an additional 3 minutes. The identical process as before was followed to prepare the control specimen, except Nano particles were not introduced. Standard-sized cubes and cylinders of 300 mm in length and 150 mm in diameter were both cast using a steel mould. The 100 × 100 × 500 mm beam moulds are also cast using a steel mould. It was decided to let the specimens cure for 28, 56, and 90 days in water after they were removed from the moulds. According to BIS standards, the specimen's standard dimensions of cubes, 150 × 300 mm cylinders, and a 100 × 100 × 500 mm beam were utilised to determine the specimen's compressive strength, indirect tensile strength, and flexural strength, respectively. Four basic supports and rectangular RC beams were to be cast and tested. Figure 1 shows the features and configuration of a beam. Cast reinforced concrete beams with a cross section of 150 × 300 mm and a span of 1500 mm were placed within the iron formwork. Two 10mm rods were used to add flexural strength to the bottom of the beams. Two 8 mm diameter rods are placed at the top for reinforcement. Each beam has 6 mm stirrups separated 100 mm c/c for shear reinforcement.

**Figure 1:** Design of beam elevation (all dimensions are mm).

3.1. Proportioning of mix design

In a traditional concrete specimen, cement, fine aggregate, and coarse aggregate were proportioned according to code IS 10262:2019 [12]. By substituting nano alumina and cement by 2% and 20% of the cement mass for normal concrete, Nano replaced concrete was prepared. Table 3 lists the various mixtures and their mix proportions that were employed in the experimental work for the various grades. The sample identifiers NC30, NA30, NC40, NA40, NC50, and NA50 each stand in for a different concrete grade, such as M30, M40, and M50.

3.2. Nano- Al_2O_3

The study used nano- Al_2O_3 particles from a local market with an average particle size of 18 and 10 nm. As shown in Figure 2, nano alumina material was mixed with cement binder in a small container using a rotary mixer. Mixing water and superplasticiser was started with an electrical mixer. After preparation of nano alumina concrete mixer, solution and modified cement were added to the other components, and the concrete mixes were poured into steel specimen models, compacted, and cured in water baths at 30–35 °C.

4. RESULTS AND DISCUSSIONS

4.1. Compressive strength

In structural design, compressive strength is the most important mechanical parameter. In regards to Table 4 and Figure 3. At 28 days, M30, M40, and M50 concrete mixes showed 10%, 28.24%, and 33.52% increases in compressive strength relative to the control mix, while at 56 days, they reached 30.25%, 44.36%, and 52.47% increases in compressive strength. At 90 days, compressive strength was increased to 32.78%, 48.55%, and 54.12%, respectively. By strengthening the bond between the aggregates and the cement paste, compression strength can be increased. This resulted in decreased porosity and increased compactness at the same time. As can also be seen in Figure 3, the compressive strength of concrete containing NC and NA increases with increasing curing time [13].

Table 3: Mix proportions for specimens.

GRADE OF CONCRETE	TYPE OF CONCRETE	CEMENT (kg/m ³)	NANO ALUMINA (kg/m ³)	FINE AGGREGATE (kg/m ³)	WATER (kg/m ³)	COARSE AGGREGATE (kg/m ³)	SP (kg/m ³)
M30	NC30	354	–	684	180	1056	–
	NA30	302	3.54	684	180	1056	3.84
M40	NC40	382	–	667	170	1162	–
	NA40	315	3.66	667	170	1162	3.91
M50	NC50	403	–	645	155	1278	1.84
	NA50	332	3.82	645	155	1278	6.22

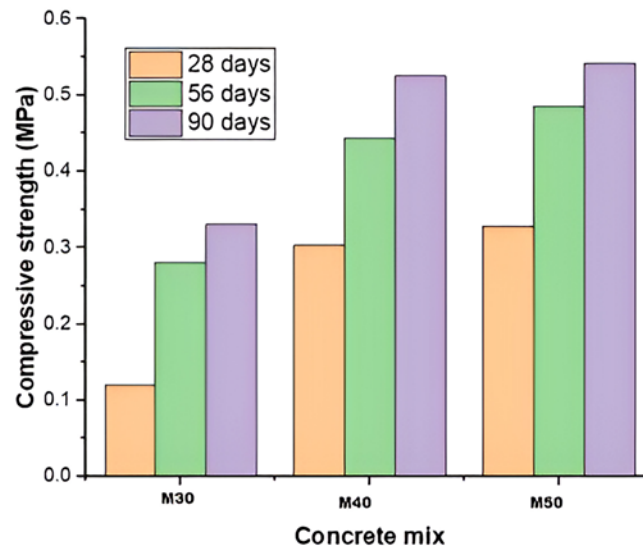
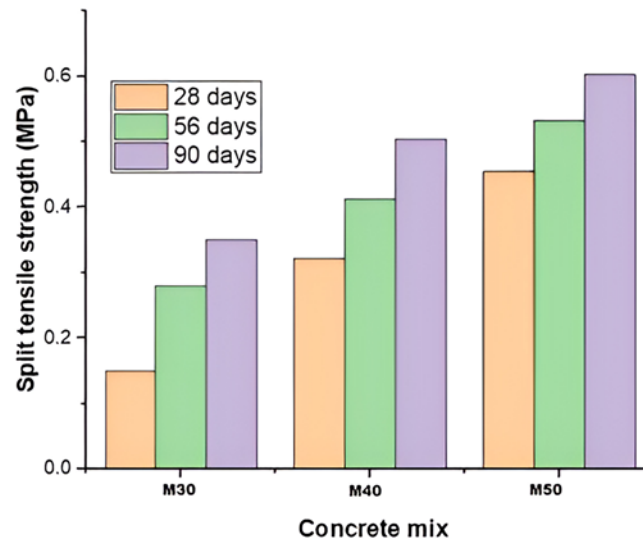
NC* – Normal Concrete; NA* – Nano Alumina Concrete



Figure 2: Nano alumina.

Table 4: Test results on changes in concrete mixes' compressive strength.

CONCRETE MIX	COMPRESSIVE STRENGTH CHANGES AT 28 DAYS	COMPRESSIVE STRENGTH CHANGES AT 56 DAYS	COMPRESSIVE STRENGTH CHANGES AT 90 DAYS
M30	+1.0	+2.8%	+3.3%
M40	+30.25%	+44.36%	+52.47%
M50	+32.78%	+48.55%	+54.12%

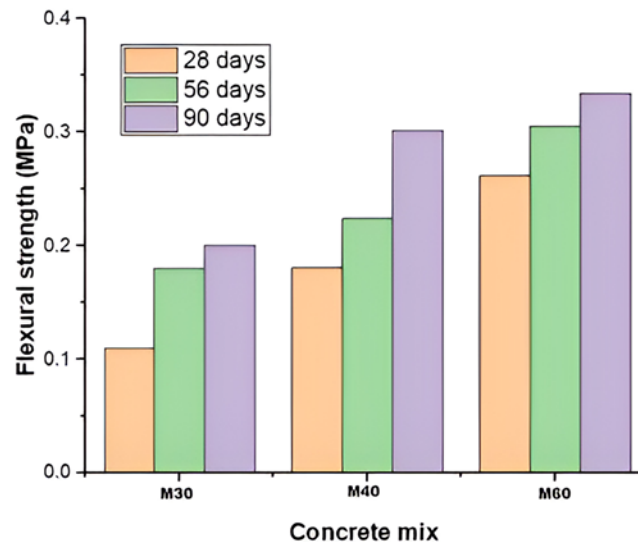
**Figure 3:** Concrete mix compaction at 28 days, 56 days, and 90 days.**Figure 4:** Concrete mix tensile strength at 28 days, 56 days, and 90 days after mixing.

4.2. Split tensile strength

As shown in Figure 4 and Table 5, all concrete mixtures including NC and NA underwent indirect tensile strength or split tensile strength tests 28, 56, and 90 days after curing. After age 28, 56, and 90 days, the tensile strength of the concrete specimen M30 containing 30% NA increased by 12.3%, 22.1%, and 29.54%. Moreover,

Table 5: Test results on changes in concrete mixes' tensile strength.

CONCRETE MIX	SPLITTING TENSILE STRENGTH CHANGES AT 28 DAYS	SPLITTING TENSILE STRENGTH CHANGES AT 56 DAYS	SPLITTING TENSILE STRENGTH CHANGES AT 90 DAYS
M30	+1.2	+2.2%	+2.9%
M40	+32.17%	+41.33%	+50.42%
M50	+45.43%	+53.19%	+60.23%

**Figure 5:** Concrete mix flexural strength at 28, 56, and 90 days of age.**Table 6:** Test results on changes in concrete mixes' Flexural strength.

CONCRETE MIX	FLEXURAL STRENGTH CHANGES AT 28 DAYS	FLEXURAL STRENGTH CHANGES AT 56 DAYS	FLEXURAL STRENGTH CHANGES AT 90 DAYS
M30	+1.1%	+1.23%	+1.54%
M40	+18.09%	+22.40%	+30.12%
M50	+26.13%	+30.51%	+33.41%

at 56 days, the Split tensile strength reached 32.17%, 41.33% and 50.42%, respectively. Furthermore, the Split tensile strength was increased at ages 90 days to 45.13%, 53.19%, and 60.23%, respectively. Overall, it can be said that the combination of NC and NA was the most effective in increasing concrete tensile strength compared to the control mix [14].

4.3. Flexural strength

All NC and NA concrete mixes are shown in Figure 5 and Table 6 for age 28 and 56 days, respectively, for the data on flexural strength and percentage increase. As concrete specimens containing NA aged from 28 to 50, their flexural strength increased by 12.3%, 22.1%, and 29.54%, respectively. Flexural strength increased to 18.09%, 22.40% and 30.12% at 56 days. At 90 days of age, Flexural strength increased from 26.13 percent to 30.51% and 33.41%. Clearly, fibers affect concrete flexural strength and protect it from quick cracking. When NS was used alone in the concrete mix, flexural strength increased slightly when compared to the control mix. Fiber use, however, resulted in an improvement in flexural strength due to the additional fiber contribution before fracture [15].

4.4. Microstructure

It is primarily the microstructure of cement-based binding materials that determines its strength and durability. The microstructure of the sample was examined using SEM. Nanoparticles retrieved harmful pores from mortar, so portions of that mortar were collected after 28, 56 and 90 days of hardening (for microstructure analysis). SEM images of mortar portions with and without nanoparticles are shown in Figure (6a). In morphological analysis, concrete pastes with nanoparticles exhibited significantly different textures than conventional concrete pastes. It can be seen in Figure 6b that the pore size of the mixture without nanoparticles was relatively large, whereas it was substantially smaller in the mixture with nanoparticles (Figure 6c). Because of the filling effect of nanoparticles present in the mixture, pores were retrieved. This resulted in an increase in mortar particle density in concrete. In the presence of different nanoparticles, the C–S–H gel rapidly formed and the size of $\text{Ca}(\text{OH})_2$ crystals decreased as the crystalline $\text{Ca}(\text{OH})_2$ was consumed [16–17]. There are needle hydrates surrounded by C–S–H gel in conventional concrete, and the crystal size is larger than that of concrete containing nanoparticles.

4.5. XRD Analyses

XRD and SEM analyses were performed on the nano- Al_2O_3 , and the resulting results are shown in Figures 7 and 6. It can be seen in Figure 7 that nano- Al_2O_3 's external surface is composed of several rough structures that do not have a uniform shape. Al_2O_3 nanoparticles have an irregular crystalline surface. In the XRD analysis, all peaks were compared, and nano- Al_2O_3 was confirmed to exist [18].

4.6. Crack pattern and mode of failure

All of the studied beam examples had the typical flexural failure, in which the steel bar gave way and the concrete was crushed by the failure loads, as shown in Figure 8, which displays the fracture pattern and method of failure of each specimen. The first fracture originated in the flexural zone and travelled to the compression zone. Even though a few shear cracks were visible under experimental loading, the beam's collapse was not caused by these cracks. Flexure caused almost all of the beams to collapse. However, the ultimate failure is brought on by concrete crushing as a result of ultimate loading [19].

When NA particles were added to the concrete mixture, a filling effect was created that reduced the overall number of cracks while improving crack spacing. All of the fractures that occurred in the beam's mid-span between the point loads were flexural cracks. All of the tensile steel bars in these specimens broke, and all of the specimens showed flexural failure, because of the comparatively low ratio of the longitudinal tensile reinforcement. As the failure load level was achieved, a few shear-bending fractures developed and spread diagonally in the direction of the point load [20].

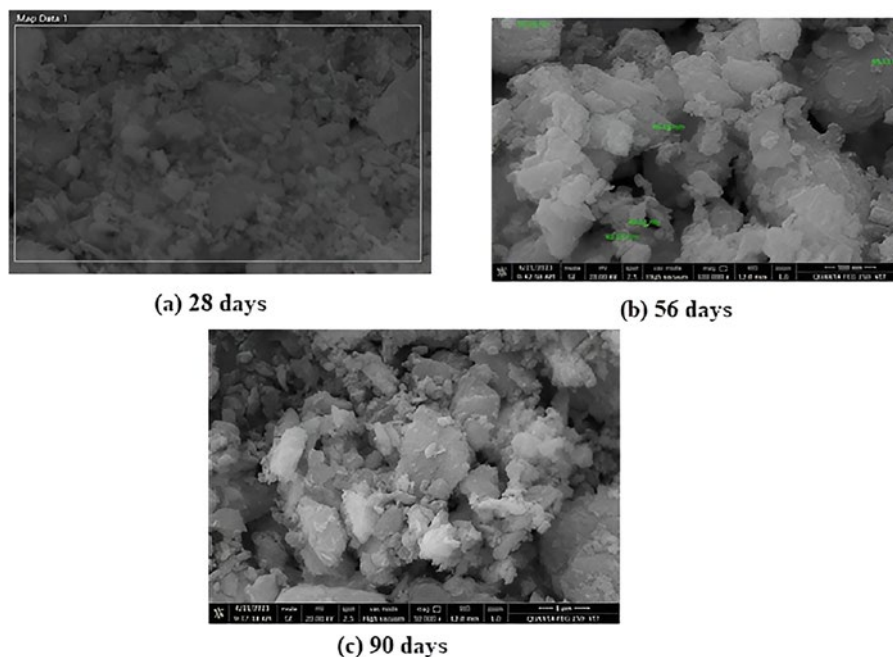


Figure 6: SEM images 28, 56 and 90 days.

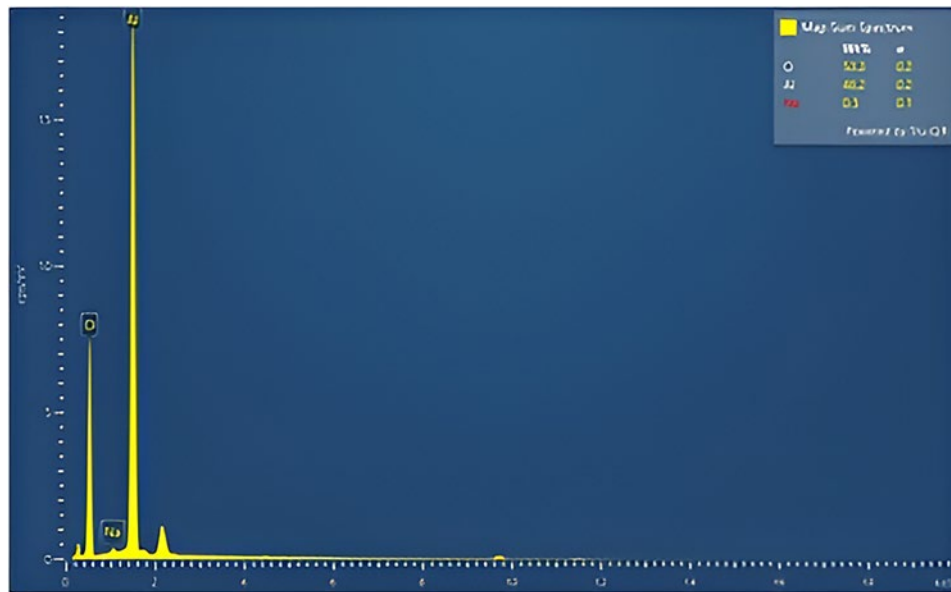


Figure 7: XRD analysis results.



Figure 8: Crack pattern and mode of failure.

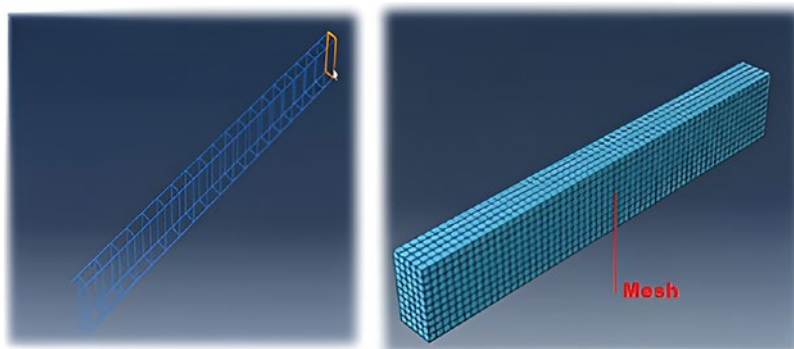


Figure 9: Assemblage of RC beam.

4.7. Finite Element Analysis with Nonlinearity

The load-carrying capability of RC beam with Nano alumina is predicted numerically using ABAQUS, a finite element programme. For the purpose of simulating the RC beam and comparing the findings experimentally, nonlinear finite element analysis was used. A constitutive model is used to simulate the nonlinear material behaviour. The failure analysis is carried out using the Finite Element programme. The element seen in Figure 9 was modelled using a continuum element with a 10 noded brick element. Three degrees of freedom at each node were given three translational degrees of freedom in order to ensure consistent stress distribution. According to Figure 9, the reinforcing bars and stirrups were modelled as three-dimensional truss components with three degrees of freedom for translation. At a distance of 100 mm on either side of the beam, pinned support was offered. The model is simulated using the concrete damaged-plasticity model from Table 7, which is employed in a nonlinear three-dimensional FE study of reinforced concrete beams. The experimental analysis is contrasted with the FE results. Steel loading plates are used to apply two-point loads in order to simulate four-point loading. The failure load, load-deflection, initial cracks, ultimate loading, and ductility were all covered by the NLFEA. Analysis that is static and non-linear was done.

4.8. Ultimate failure load for analysis

Compared to beams enhanced by nanoparticles, the stiffness of controlled reinforced concrete is significantly lower. On the beam's middle span, the deflection was noted. From Figure 10(a,b) and Figure 11(a,b), it was shown that the load-displacement for both finite element and experimental analysis was consistent with the findings of the experiments in both nano-alumina. Experimental results showed that the load-displacement curve in finite element analysis started off linear. Experimentally, the maximum failure for Group 1 beam NC was determined to be 142 kN, whereas analytic analysis for the same specimen revealed a 167 kN maximum failure, as shown in Table 7. The final failure load for the second set of beam NA was measured to be 165 kN, while

Table 7: FEA results of beam.

CATEGORY	YIELD LOAD kN	FAILURE LOAD kN	INITIAL DEFLECTION mm	FINAL DEFLECTION mm	DUCTILITY INDEX %
NC30	53	142	1.3	3.9	29.54
NC40	24	93	1.7	7.0	22.5
NC50	48	167	1.0	3.5	30.17
NA30	61	165	1.3	3.7	34.28
NA40	32	134	1.9	6.3	28.54
NA50		175	1.4	3.4	39.51

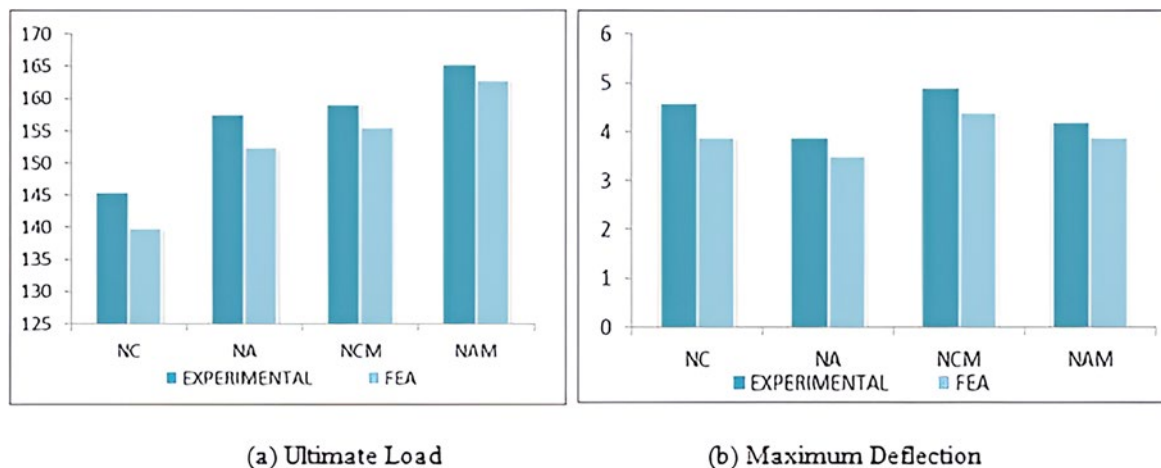


Figure 10: Results from experiments and analyses are compared.; (a) Ultimate load (b) Maximum deflection.

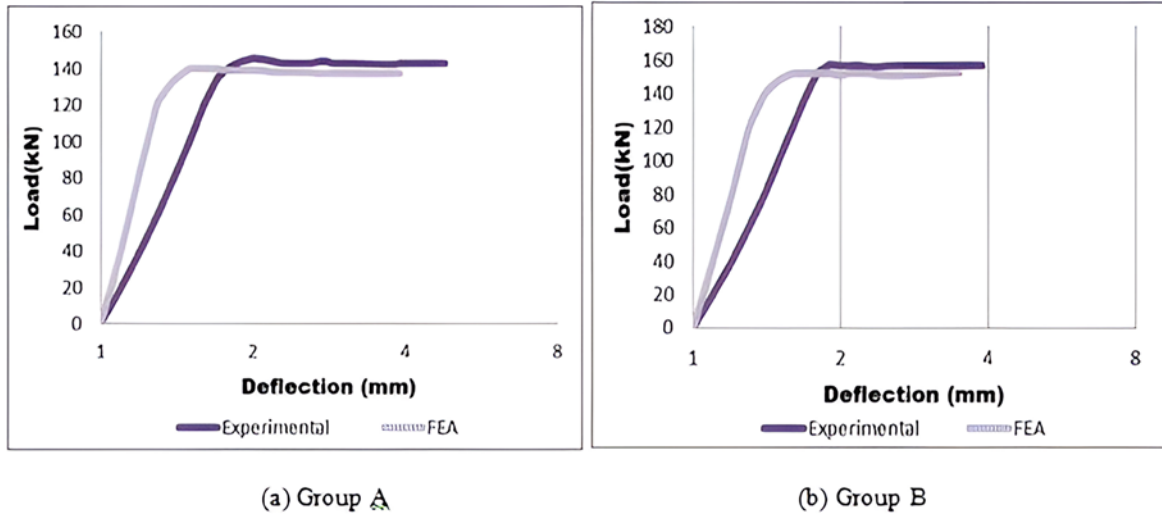


Figure 11: Analytical and experimental load-deflection comparison (a) Group A; (b) Group B.

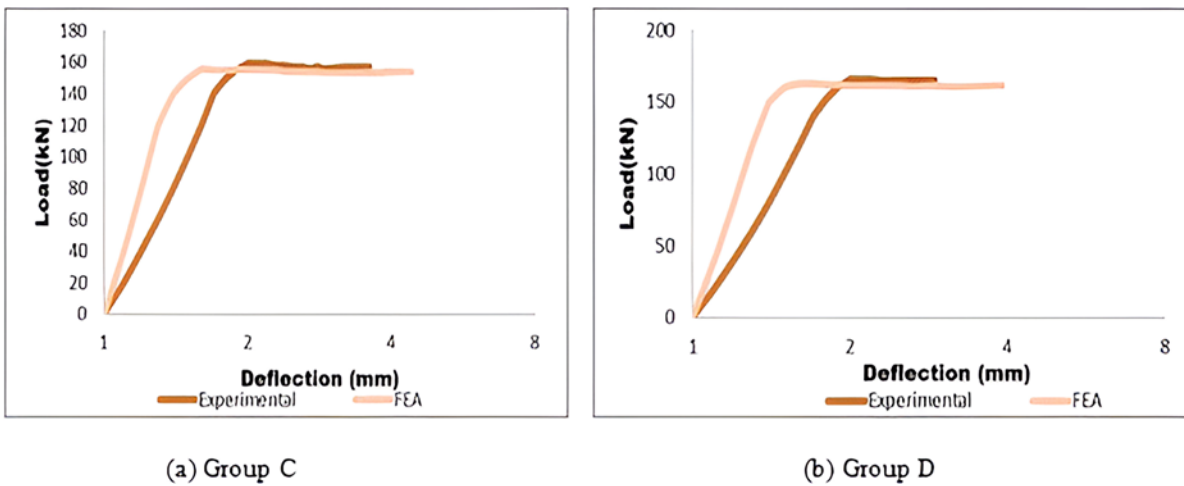


Figure 12: Analytical and experimental load-deflection comparison (a) Group C; (b) Group D.

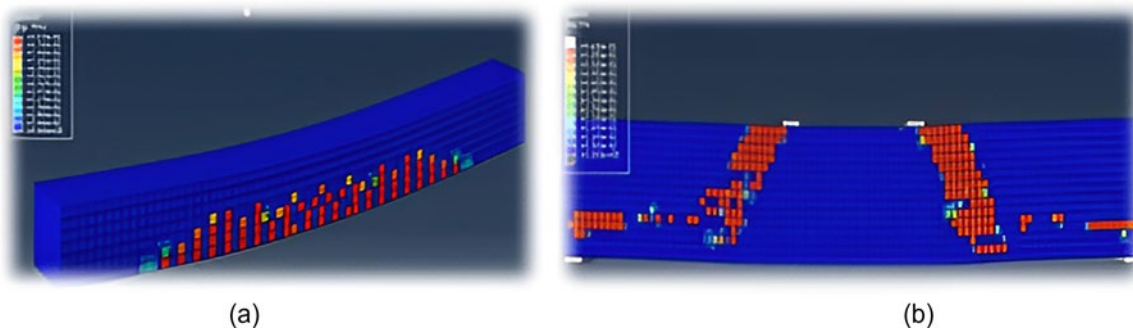


Figure 13: (a) Crack pattern in NA specimen (b) Concrete damage at compression.

Table 8: FEA results of beam

CATEGORY	ULTIMATE LOAD kN		ULTIMATE DEFLECTION kN		P_{FEA}/P_{EXP}	$\delta_{FEA}/\delta_{EXP}$
	EXPERIMENTAL	FEA	EXPERIMENTAL	FEA		
NC	148.7	140.3	5.1	4.5	0.95	0.84
NA	155.2	148.6	3.7	3.3	0.96	0.90
NCM	161.5	159.5	5.0	4.2	0.96	0.89
NAM	173.6	166.7	4.9	4.3	0.97	0.91

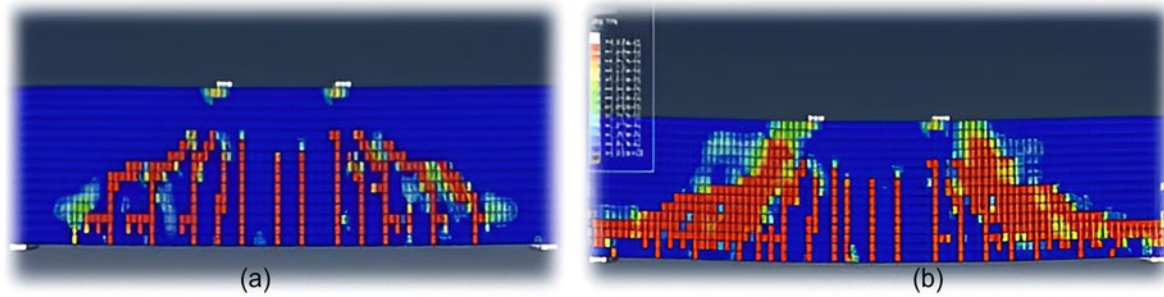


Figure 14: (a) Crack pattern in tensile zone (b) Concrete damage at tension.

the failure load predicted by analysis was 175 kN. The tensile property of the concrete is also improved by the material property, which also improves the flexural property of the RC beam (Figure 12 (a,b))

4.9. A deflection and failure mode

In ABAQUS, a simulation model was created to ascertain the beam's deflection and cracking pattern. Figure 13(a, b) depicts the fracture and tensile damage to the beam NA. The area of the beam that sustains the most damage is below the loading point and in the middle of the beam's span. According to Figure 13(a), the break spans up to 50% of the beam. Since the loading locations are a zone of continuous bending moment, as shown in Figure 13(b), it is noted that the fractures occurred there. Analytical and experimental representations of beam deflection are shown in Table 8. Experimentally, Beam NC had a 1.3 mm beginning deflection and a 3.5 mm final deflection; however, analytical analysis revealed that the deflection was really 3.6 mm. Additionally, the vertical deflection was determined to be 3.0 mm experimentally but was seen to be 3.3 mm NA. As demonstrated in Figures 10(a) and 10(b), the similar variance was seen in beams NC and NA as well. According to Figure 8, the comparison between the NLFE and experimental methods was generally acceptable. Fig. depicts the comparative load-deflection curve. Analytical and experimental results are compared for the beam's deflection. For NC, NA, NCM, and NAM, the $\delta_{FEA}/\delta_{EXP}$ values were 0.84, 0.90, 0.89, and 0.91, respectively. The crack patterns are comparable as well. From the mid-span to the loading point, there were fissures. The breaking patterns are in line with the beams' testing findings as well (Figure 14 (a,b)).

5. CONCLUSIONS

The following observations and deductions are made in light of the findings of the experiments conducted on samples of conventional concrete and Nano alumina concrete:

- With partial substitution of Nano alumina at 28, 56, and 90 days for M30, M40, and M50, it is discovered that the compressive strength of Nano modified concrete is enhanced to a maximum value of 10%, 28.24% and 33.52%, 30.25%, 44.36% and 52.47%, and 32.78%, 48.55%, and 54.12% in comparison to control specimen.
- It is discovered that nano-modified concrete has boosted split tensile strength to maximum values of 12.3%, 22.1%, and 29.54%. When Nano alumina was partially substituted for the control specimen at 28, 56, and 90 days for M30, M40, and M50, the results were 32.17%, 41.33%, and 50.42% and 45.13%, 53.19%, and 60.23%.

- With the partial substitution of Nano alumina with respect to control specimen at 28, 56, and 90 days for M30, M40, and M50, it is discovered that the flexural strength of Nano modified concrete is increased to a maximum value of 12.3 MPa, 22.1 MPa, 29.54 MPa, 18.09 MPa, 22.40 MPa, and 30.12 MPa, as well as 26.13 MPa, 30.51 MPa, and 33.41 MPa.
- Due to the large specific area of particles with a size of 20 Nm, nanoparticles played a significant role in the improvement of strength. The early age development of concrete strength is enhanced by the application of nano alumina.
- By eating it in a pozzolanic reaction, the effect of nano alumina will both enhance the microstructure and reduce the concentration of free calcium hydroxide.
- Concrete's microstructure may be changed to enhance its mechanical capabilities and lengthen its useful life, both of which support the development of a sustainable built environment.
- To compare the results analytically, a nonlinear finite element model was simulated using a nonlinear beam response reinforced by nano-silica and produced sand. The simulated model retrieved behaviour that was consistent with that of the experimental beam. It was discovered that the average load agreements between P_{FEA}/P_{Exp} and $\delta_{FEA}/\delta_{Exp}$ were 0.96 and 0.85, respectively. The experimental findings and the deflection, fracture pattern, and concrete damage under tension and compression were in good agreement. Consequently, confirm the simulation model's correctness.

Future research should focus on expanding the experimental scope by testing various concentrations of nano-Alumina and applying these findings to different structural elements, such as columns or slabs. Furthermore, investigating the environmental sustainability of nano-Alumina, including its impact on carbon footprint reduction and life-cycle costs, could lead to further improvements in concrete technology.

6. BIBLIOGRAPHY

- [1] SMIRNOVA, O.M., MENENDEZ-PIDAL, I., ALEKSEEV, A.V., *et al.*, "Strain hardening of polypropylene microfiber reinforced composite based on alkali-activated slag matrix", *Materials*, v. 15, n. 4, pp. 1607, 2022. doi: <http://doi.org/10.3390/ma15041607>. PubMed PMID: 35208146.
- [2] EL-MANDOUH, A.M., KALOOP, M.R., HU, J.-W., *et al.*, "Shear strength of nano silica high-strength reinforced concrete beams", *Materials*, v. 15, n. 11, pp. 3755, 2022.
- [3] RASHMI, R., PADMAPRIYA, R., "Experimental and analytical study on flexural behavior of reinforced concrete beams using nano silica", *Materials Today: Proceedings*, v. 50, pp. 57–69, 2021. doi: <http://doi.org/10.1016/j.matpr.2021.04.127>.
- [4] ZHANG, P., ZHANG, H., CUI, G., *et al.*, "Effect of steel fiber on impact resistance and durability of concrete containing nano-SiO₂", *Nanotechnology Reviews*, v. 10, n. 1, pp. 504–517, 2021. doi: <http://doi.org/10.1515/ntrev-2021-0040>.
- [5] RAHMANI, K., GHAEMIAN, M., HOSSEINI, S.A., "Experimental study of the effect of water to cement ratio on mechanical and durability properties of Nano-silica concretes with Polypropylene fibers", *Scientia Iranica*, v. 26, n. 5, pp. 2712–2722, 2019. doi: <http://doi.org/10.24200/sci.2017.5077.1079>.
- [6] AKBARPOUR, S., DABBAGH, H., TAVAKOLI, H.R., "The effects of steel fiber and Nano-SiO₂ on the cyclic flexural behavior of reinforced LWAC beams", *KSCE Journal of Civil Engineering*, v. 22, n. 10, pp. 3919–3930, 2018. doi: <http://doi.org/10.1007/s12205-017-0920-3>.
- [7] AMIN, M., ABU EL-HASSAN, K., "Effect of using different types of nano materials on mechanical properties of high strength concrete", *Construction & Building Materials*, v. 80, pp. 116–124, 2015. doi: <http://doi.org/10.1016/j.conbuildmat.2014.12.075>.
- [8] KHALKHALI, A., DAGHIGHI, S. "Optimum design of a coir fiber biocomposite tube reinforced with nano silica and nano clay powder", *International Journal of Engineering Transactions C*, v. 30, n. 12, pp. 1894–1902, 2017. doi: <https://doi.org/10.5829/ije.2017.30.12c.11>.
- [9] MUSTAFA, T.S., EL HARIRI, M.O., KHALAFALLA, M.S., *et al.*, "Application of nanosilica in reinforced concrete beams," *Proceedings of the Institution of Civil Engineers-Structures and Buildings*, v. 175, n. 5, pp. 363–372, 2020. doi: <https://doi.org/10.1680/jstbu.19.00170>.
- [10] SRIDHAR, J., VIVEK, D., JEGATHEESWARAN, D., *et al.*, "Mechanical and flexural behaviour of high performance concrete containing Nano Silica", *International Journal of Engineering and Advanced Technology*, v. 9, n. 2, pp. 2017–2023, 2020. doi: <http://doi.org/10.35940/ijeat.B3164.129219>.

- [11] MAJEED, Z.H., TAHA, M.R., “The effects of using nanomaterials to improvement soft soils”, *Saudi Journal of Engineering and Technology*, pp. 58–63, 2016. doi: <http://doi.org/10.21276/sjeat.2016.1.3>.
- [12] ZHANG, G., ““Soil nanoparticles and their influence on engineering properties of soils”, *New Peaks in Geotechnics*, v. 173, pp. 1–13, 2007. doi: [http://doi.org/10.1061/40917\(236\)37](http://doi.org/10.1061/40917(236)37).
- [13] MOSALMAN, S., RASHAHMADI, S., HASANZADEH, R. “The effect of TiO₂ nano particles on mechanical properties of poly methyl metacrylate nanocomposites”, *International Journal of Engineering Transactions B*, v. 30, n. 5, pp. 807–813, 2017. doi: <http://doi.org/10.5829/idosi.ije.2017.30.05b.22>.
- [14] LEE, J., MAHENDRA, S., ALVAREZ, P., “Nanomaterials in the construction industry: a review of their applications and environmental health and safety considerations”, *ACS Nano*, v. 4, n. 7, pp. 3580–3590, 2010. doi: <http://doi.org/10.1021/nn100866w>. PubMed PMID: 20695513.
- [15] KRISHNAVENI, C., SENTHIL SELVAN, S., “Study on nano-alumina in concrete”, *Materials Today: Proceedings*, v. 46, n. Part 9, pp. 3648–3652, 2021. doi: <http://doi.org/10.1016/j.matpr.2021.01.809>.
- [16] KHALDI, M., BOUZIANE, M.M., BOUGHERARA, H., *et al.*, “Experimental and numerical analysis of the mechanical behavior of bone cement reinforced with alumina particles”, *Journal of the Brazilian Society of Mechanical Sciences and Engineering*, v. 45, n. 7, pp. 372, 2023. doi: <http://doi.org/10.1007/s40430-023-04283-x>.
- [17] ORMAN SUBASI, R., CAGLAR, N., DEMIRTAS, G., *et al.*, ““Nonlinear finite element study on the improvement of torsional strengthening of RC beams with diagonal shear reinforcement”, *Journal of Construction*, v. 23, n. 3, pp. 480–496, 2024. doi: <http://doi.org/10.7764/RDLC.23.3.480>.
- [18] NEMATZADEH, M., ARJOMANDI, A., FAKOOR, M., *et al.*, “Pre-and post-heating bar-concrete bond behavior of CFRP-wrapped concrete containing polymeric aggregates and steel fibers: experimental and theoretical study”, *Engineering Structures*, v. 321, pp. 118929, 2024. doi: <http://doi.org/10.1016/j.eng-struct.2024.118929>.
- [19] SHARIATI, M., POURTEYMURI, M., NAGHIPOUR, M., *et al.*, “Evolution of confinement stress in axially loaded concrete-filled steel tube stub columns: study on enhancing urban building efficiency”, *Sustainability*, v. 16, n. 17, pp. 7544, 2024. doi: <http://doi.org/10.3390/su16177544>.
- [20] SABETIFAR, H., FAKHARI, M., NIKOFAR, M., *et al.*, “Comprehensive study of eccentrically loaded CFRP-confined RC columns maximum capacity: prediction via ANN and GEP”, *Multiscale and Multidisciplinary Modeling, Experiments and Design*, v. 8, n. 3, pp. 158, 2025. doi: <http://doi.org/10.1007/s41939-025-00738-x>.